Partial and perfect dislocation nucleation at the onset of stress relaxation in $In_{0.60}Ga_{0.40}As$ active layers of high mobility transistors grown on InP

F. Peiró,[a] A. Cornet, and J. R. Morante
LCMM. Departament Física Aplicada i Electrònica, Diagonal 645-647, 08028 Barcelona, Spain

(Received 12 October 1994; accepted for publication 23 January 1995)

The morphology of compressive $In_xGa_{1-x}As/In_{0.52}Al_{0.48}As$ layers grown on (100)-InP substrates by molecular beam epitaxy was observed by transmission electron microscopy. A preliminary analysis of the network of misfit dislocations at the interface in layers with a thickness of 0.5 μm and x_{In} between 54% and 63% led to a further study of the onset of stress relaxation for layers with composition $x_{In}=60\%$ and thickness ranging from 5 to 25 nm. A critical thickness was found for plastic relaxation at 20 nm$<t_c<$25 nm. Following a model of excess stress, a mechanism for the nucleation of dislocations according to the sequence 90°partial→60°perfect→30°partial is proposed.© *1995 American Institute of Physics.*

I. INTRODUCTION

The determination of the onset of plastic relaxation of strained layers in mismatched systems is important in demonstrating the reliability of the devices based on these heterostructures. Most transmission electron microscopy studies on this subject refer mainly to systems such as Ge_xSi_{1-x}/Si,[1–3] GaAs/Si,[4–6] and $In_xGa_{1-x}As/GaAs$,[7–9] whereas research on $In_xGa_{1-x}As/In_yAl_{1-y}As/InP$ is scarce.[10,11] The main aim of our research was to study the growth of these heterostructures for application in high electron mobility transistors (HEMT).[12] Hence, following a detailed study of the optimization of the growth of the $In_{0.52}Al_{0.48}As$ buffer layer,[11] this article describes the characterization of strained $In_xGa_{1-x}As$ layers, constituting the active well for carrier confinement in HEMT devices. It was not our purpose to perform a complete transmission electron microscopy (TEM) analysis of the critical thickness values (t_c) according to the initial mismatch, since on the one hand the wide range of In compositions (x_{In}) and epilayer thicknesses (t) and on the other the amount of work involved (both thin foil preparation and observation) make TEM unsuitable. Other techniques such as double crystal x-ray diffraction[13] allow faster determination of t_c in much wider domains of x_{In} and t. However, TEM is the only technique that reveals the nature of the defect, and is hence an essential tool for the observation of the initial steps of the relaxation process.

Here, we present the results of a study of the stress relaxation mechanisms in $In_{0.60}Ga_{0.40}As$ layers. We show that, according to the excess-stress model of Dodson *et al.*[14] the strain relaxation starts by the nucleation of 90° Shockley partial dislocations, followed by perfect ones 60° in character, and finally the 30° partials, giving rise to a mixed configuration (stacking faults and misfit dislocation network) in the first steps of the relaxation and evolving fast to a perfect network of dislocations at the interface as layer thickness increases.

[a]Also with: Serveis Científico-Tècnics, Lluís Solé i Sabarís 1-3, 08028 Barcelona, Spain.

II. RESULTS AND DISCUSSION

Initially, four $In_xGa_{1-x}As$ layers with the same thickness ($t=0.5$ μm) but different In molar fractions ranging from 54.1% to 62.5%, were grown on (100) InP, with a corresponding initial lattice mismatch (f) between 9×10^{-4} and 6.5×10^{-3} (see Table I). The growth temperature was fixed at 515 °C. For samples AL954 and AL955 no evidence of strain relaxation was observed. In contrast, in both AL957 and AL958 a network of misfit dislocation was observed at the layer/substrate interface, increasing in density for higher lattice mismatch. The evolution of dislocation density as x_{In} rises is illustrated in Fig. 1. The dislocations lines lie parallel to [011] and [01$\bar{1}$] directions. Since the images were obtained in bright field two beam conditions with the operating reflections $g=\langle022\rangle$ and $g=\langle040\rangle$ of the (100) zone axis and extinction of the dislocation contrast was not obtained for any of these reflections, we can thus conclude that the dislocations are 60° in nature, with Burger vector $b=a/2$ $\langle011\rangle$. A clear anisotropy in the distribution of dislocation along the directions [01$\bar{1}$] and [011] is also remarkable. Such anisotropy has been extensively reported in several III-V systems and has been related to differences in Peierls friction barriers between the {1$\bar{1}$1}-[011] and {1$\bar{1}$1}-[01$\bar{1}$] gliding systems.[15] Finally, it should be emphasized that a complex defect configuration was observed in some regions (Fig. 2). A dislocation line at the interface often turned into a threading segment propagating towards the layer surface (labeled TD on Fig. 2), or it was pinned by a stacking fault (labeled SF). Finally, some extended dislocation loops gliding on the {111} planes were also present (labeled DL).

Taking into account the layer/substrate mismatch, if the layers were completely relaxed the dislocation should appear at an average distance, p, of 470 Å for sample AL957 and 320 Å for AL958 (mismatch $f=0.45\%$ and $f=0.65\%$, respectively). However, the experimental measurements show higher values of p: 6200 and 2500 Å. Assuming that all the dislocations contribute to the stress relaxation, we can conclude that the layers have a remaining strain of 91% and 88%, respectively. Nevertheless, Dixon *et al.*[16] have shown that some dislocation configurations [like that arrowed on Fig. 1(c)] may correspond to dislocation dipoles with oppo-

Downloaded 10 Jun 2010 to 161.116.168.169. Redistribution subject to AIP license or copyright; see http://jap.aip.org/jap/copyright.jsp

TABLE I. Characteristics of the $In_xGa_{1-x}As$ layers: x_{In} is the molar fraction of In, f is the intrinsic lattice mismatch defined as $(a_{InGaAs}-a_{InP})/a_{InP}$ and p the experimental averaged distance between misfit dislocations at the interface.

Sample	x_{In} (%)	f (%)	p (nm)
AL954	54.1	0.09	...
AL955	54.6	0.11	...
AL957	59.6	0.45	620
AL958	62.5	0.65	250

site Burger vectors, whose contribution to stress removal would annihilate, and then it is still possible for the layers to retain a higher remaining strain than the values indicated.

Having established that the relaxation process starts at a certain thickness below 0.5 μm in layers with In composition of 0.60, we grew a second group of samples with fixed composition $x_{In}=60\%$ and thicknesses ranging from 5 to 25 nm in steps of 5 nm. In this case, however, the InGaAs was grown on an $In_{0.52}Al_{0.48}As$ buffer so as to avoid additional contributions to the layer stress, such as the strain induced by the presence of an InAs interfacial layer on the InP formed during the thermal cleaning of the substrate due to the P-As exchange.[17] No evidence of strain relaxation for InGaAs thickness up to 20 nm was observed for these layers. In contrast, the relaxation process has started for the 25 nm layer, for which the TEM images reveal the morphology of the layer at the onset of the relaxation (Fig. 3; operating reflection $g=022$). We observe the presence of 60° dislocations irregularly distributed on the layer surface, coexisting with stacking faults (SF on the micrographs) and threading dislocations (TD). During the observation, a local increment in the foil temperature caused by focusing the electron beam induced the activation of the dislocation motion, which annihilated the stacking faults and favored further propagation of the resulting threading segments as 60° perfect dislocations. This process can be followed by observing the frozen configurations (numbered 1–4) in Fig. 3.

Let us now discuss the origin of such a complex configuration. We can suppose that perfect 60° dislocations nucleate first, and then dissociate into two Shockley partials according to the reaction:

$$a/2[\bar{1}10]=a/6[\bar{1}21](30°)+a/6[\bar{2}1\bar{1}](90°).$$

This dissociation is energetically favored, taking into account the dependence of the related energy on b^2:

$$E=\left[\frac{Gb^2\sin^2\theta}{4\pi(1-\nu)}+\frac{Gb^2\cos^2\theta}{4\pi}\right]\ln\left(\frac{R}{r_o}\right), \quad (1)$$

where b is the Burger vector module of the dislocation and θ is the angle it forms with the growth surface. Following the model of Mareé *et al.*[18] the dissociation of a 60° dislocation in a tensile stress field gives rise to a 90° leading partial, immediately followed by the trailing 30° partial. Since the dislocation line lies along the direction of the stress for the 90° partial, the force acting on the leading partial is stronger, and they remain dissociated leaving a stacking fault between them. Conversely, in a compressive stress field (which is our

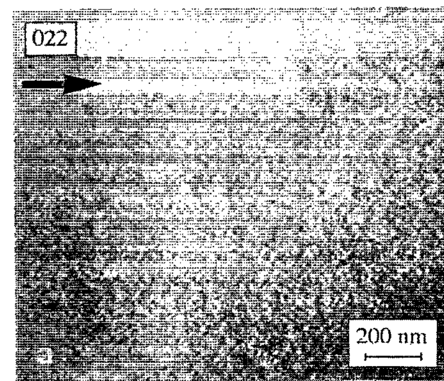

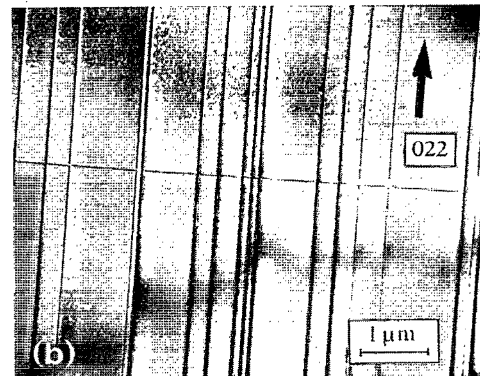

FIG. 1. Plan view images of the $In_xGa_{1-x}As$ layers on the (100) zone axis. The arrows show the reflection used to perform the bright field strong two-beam conditions, (a) $x_{In}=54\%$. The layer remains totally strained judging from the total absence of defects in the layer; (b) $x_{In}=59.6\%$, we observe an orthogonal array of perfect 60° misfit dislocations lying along the ⟨011⟩ directions; (c) $x_{In}=62.5\%$, the density of misfit dislocations has increased. In both (b) and (c) a clear asymmetry of dislocations distribution along [011] and $[01\bar{1}]$ is remarkable.

case), the leading partial is of 30° nature and the trailing one is the 90° partial. Consequently, when the 30° partial appears, the 90° partial follows immediately and since it propagates faster it traps the leading partial and annihilates the stacking fault. However, this mechanism contradicts our experimental results. We conclude then that the partial dislocations (and hence the stacking faults) do not arise from dissociation of perfect dislocations, but rather that they must nucleate independently. Let us now assume that the partial dislocations nucleate first. The separation between the 30° and 90° partials leads to the formation of a stacking fault

Downloaded 10 Jun 2010 to 161.116.168.169. Redistribution subject to AIP license or copyright; see http://jap.aip.org/jap/copyright.jsp

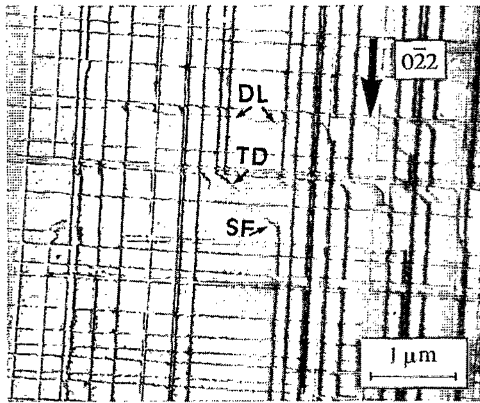

FIG. 2. Bright field $g=0\bar{2}2$ image of the $In_{0.63}Ga_{0.37}As$ layer. Among the misfit dislocation network, we can remark the presence of threading segments propagating up to the top of the layer (TD), misfit dislocations pinned at stacking faults (SF) and dislocation loops on {111} planes (DL).

with an energy γ_{SF}. This contribution should be taken into account in order to determine whether the energy balance in the system allows the nucleation of the partials. Recently, Lee *et al.*[19] analyzed the probability of nucleation for Lomer, 60° and partial dislocations in the GaAs/Si system, as a function of $\Delta\epsilon/\Delta E$ (where ϵ is the strain in the layer). They showed that although the Lomer (90° pure edge) is the most effective for strain relaxation, the most frequent dislocations are those whose nucleation barrier is lower (in this case, the 90° partial), due to kinetic limitations in the molecular beam epitaxy (MBE) process. Hull *et al.*[20] have also reported that in the compressive system Ge_xSi_{1-x} on (011) Si substrates, the critical thickness for the nucleation of the 90° partial with $b=a/6\ \langle 112\rangle$ is lower than the critical thickness for the 60° dislocations. However, these authors also remark that the opposite occurs in the case of growth on exact (100)-Si substrates. According to the model of Dodson and Tsao, the excess stress σ_{ex} (which is the driving force for the nucleation and motion of dislocations) is determined by a balance between the stress due to the elastic strain, the stress associated with the dislocation line itself, and the contribution of the stacking fault energy if the dislocations concerned are partial:

$$\sigma_{ex}=2\mu\epsilon S_\theta\frac{(1+\nu)}{(1-\nu)}-\frac{\mu b\cos\phi(1-\nu\cos^2\theta)}{4\pi t(1-\nu)}\times\ln\left(\frac{\alpha t}{b}\right)-\frac{\gamma}{b}, \quad (2)$$

where S_θ is the Smith factor of the dislocation, ϵ is the layer strain, t the layer thickness, α a parameter related to the dislocation core, and γ the stacking fault energy. If we calculate this excess stress taking[19] α as 2 and the elastic moduli μ (shear stress) and ν (Poisson ratio) for a composition $x_{In}=60\%$ by linear interpolation between the InAs and GaAs values,[21] and assuming $\epsilon=f$, then a dislocation of 60° would see an excess stress of 1.8×10^8 dyn/cm^2 whereas a 90° partial would see an stress of 1.3×10^9 dyn/cm^2, without taking into account γ_{SF} in the latter case. Kim *et al.*[21] have reported that the additional energy of the stacking fault coming from the partial nucleation is far lower than the energy of the 90° or 60° dislocations.

These results suggest that at the onset of strain relaxation and for relatively small layer thickness, it is possible for the 90° partial dislocation to nucleate and propagate, leaving a stacking fault behind, since its associated energy is still low.[19,22] As t increases, the excess stress for the 60° dislocation rises and the excess stress for the 90° partial falls due to the contribution of γ_{SF}. However, the limit for the nucleation of a 30° partial is still not reached. This situation would give rise to a configuration like that observed in Fig. 3, i.e., coexistence of 60° and 90° partial dislocations. For higher t, the contribution of the term γ_{SF} rises, and then the systems tends to annihilate the stacking fault by the nucleation of the 30° partial. This is only possible if t is high enough or if the energy is locally increased (as it is if we converge the electron beam on the foil surface). Then the stacking fault disappears by the recombination 30°+90°, giving rise to a 60° segment which may glide on the {111} planes leading to new dislocation lines at the interface. Then, as layer thickness increases, the density of 60° dislocations may be higher and the ρ_{SF} may decrease, leading to a configuration like that of Fig. 1(c). In order to test this proposed mechanism, we can calculate the expected critical thickness t_c for all the dislocations from Eq. (2) at the limit $\sigma_{ex}=0$. Assuming a value $\gamma_{SF}=25$ mJ/m[19,23] the results are $t_c^{90°}$ = 210 Å, $t_c^{60°}$ = 228 Å, and $t_c^{30°}$ = 234 Å. Consequently, the order of dislocation nucleation should be 90°-60°-30°. The main point to remark is the perfect correspondence of the t_c^i values with the results of the TEM observation 20 nm$<t_c<$25 nm, showing good agreement with the model of Dodson and Tsao.[13,22] Nevertheless, we must also point out that the t_c^i values are close to each other and depend strongly on the γ_{SF} considered. Hence, once the first t_c has been overcome the system should evolve fast, developing a network of perfect 60° misfit dislocations at the interface, like that shown in Fig. 1.

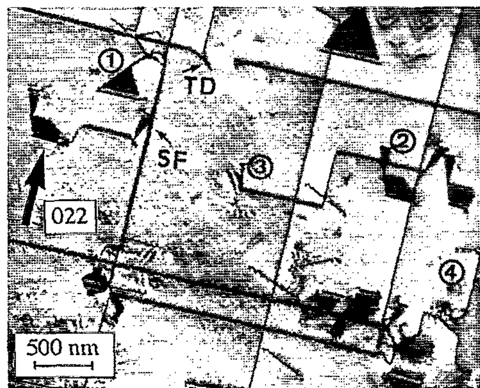

FIG. 3. Bright field $g=022$ image along the (100) orientation of a $In_{0.60}Ga_{0.40}As$ layer 25 nm thick. We observe an irregular distribution of misfit dislocations segments at the interface frequently limited by threading segments (TD) or stacking faults (SF). The numbers show different arrangement of the defects according to the nucleation of dislocations in the order 90°(partial+SF)-60°-30° (recombination with 90° and annihilation of SF).

Downloaded 10 Jun 2010 to 161.116.168.169. Redistribution subject to AIP license or copyright; see http://jap.aip.org/jap/copyright.jsp

III. CONCLUSIONS

In summary, we have determined by TEM observations that the critical thickness for plastic relaxation of compressive $In_{0.60}Ga_{0.40}As$ is 20 nm$<t_c<$25 nm, in good agreement with the model of excess stress of Dodson and Tsao.[13,22] The 25 nm layers at the initial steps of stress relaxation present a complex morphology, showing an irregular distribution of 60° dislocations (misfit lines at the interface and threading segments) and also partial dislocations bordering stacking faults. We have proposed a mechanism for strain relaxation by initial nucleation of 90° partials and the formation of a stacking fault, considering its energy low at the onset of relaxation. The nucleation of a perfect 60° dislocation follows, and as the layer thickness increases, the limit for the nucleation of the 30° partial is overcome. Thus, the stacking faults are eliminated by recombination and threading segments originate, which in turn lead to new 60° dislocations at the interface by gliding on the {111} planes. Finally we can conclude that the mechanism of stress relaxation in these compressive layers seems to be governed by the energy barriers for dislocation nucleation.

ACKNOWLEDGMENT

This work was funded by the Spanish "Programa de Ciencia de Materiales" project under Contract Number MAT93-0564.

[1] E. P. Kvam, D. J. Eaglesham, D. M. Maher, C. J. Humphreys, J. C. Bean, G. S. Green, and B. K. Tanner, Mater. Res. Soc. Symp. Proc. **104**, 623 (1988).
[2] D. J. Eaglesham, E. P. Kvam, D. M. Maher, C. J. Humphreys, and J. C. Bean, Philos. Mag. A **59**, 1059 (1989).
[3] K. Rajan and M. Denhoff, J. Appl. Phys. **62**, 1710 (1987).
[4] C. Choi, N. Otsuka, G. Munns, R. Houdre, H. Morkoç, S. L. Zhang, D. Levi, and M. V. Klein, Appl. Phys. Lett. **50**, 992 (1987).
[5] H. L. Tsai and Y. C. Kao, J. Appl. Phys. **67**, 2862 (1990).
[6] A. Vilà, A. Cornet, A. Herms, J. R. Morante, Y. González, L. González, and F. Briones, Mater. Lett. **11**, 155 (1991).
[7] K. Rajan, R. Devine, W. T. Moore, and P. Maigné, J. Appl. Phys. **62**, 1713 (1987).
[8] K. R. Breen, P. N. Uppal, and J. S. Ahearn, J. Vac. Sci. Technol. B **7**, 758 (1989).
[9] E. A. Fitzgerald, D. G. Ast, P. D. Kirchner, G. D. Pettit, and J. M. Woodall, J. Appl. Phys. **63**, 693 (1988).
[10] L. Lazzarini, L. Nasi, C. E. Norman, G. Salviati, and S. Bertoni, J. Cryst. Growth **126**, 133 (1993).
[11] G. Wagner, V. Gottschalch, H. Rhan, and P. Paufler, Phys. Status Solidi **112**, 519 (1989).
[12] A. Georgakilas, G. Halkias, A. Christou, N. Kornilios, C. Papavassiliou, K. Zekentes, G. Konstantinidis, F. Peiró, A. Cornet, S. Ababou, A. Tabata, and G. Guillot, J. Electrochem. Soc. **140**, 1503 (1993).
[13] B. R. Bennet and J. A. Del Alamo, Proceeding of the XVIth International Conference on InP and Related Materials, 1992, p. 650.
[14] J. Y. Tsao, B. W. Dodson, S. T. Picraux, and D. M. Cornelison, Phys. Rev. Lett. **59**, 2455 (1987).
[15] B. A. Fox and W. A. Jesser, J. Appl. Phys. **68**, 2739 (1990).
[16] R. H. Dixon and P. J. Goodhew, J. Appl. Phys. **68**, 3163 (1990).
[17] G. Holliger, D. Gallet, M. Gendry, C. Santinelli, and P. Viktorovitch, J. Vac. Sci. Technol. B **8**, 832 (1990).
[18] P. M. J. Marée, J. C. Barbour, J. F. van der Veen, K. L. Kavanagh, C. W. T. Bulle-Lieuwma, and Viegers, J. Appl. Phys. **62**, 4413 (1987).
[19] H. P. Lee, X. Liu, K. Malloy, S. Wang, T. George, E. Weber, and Z. L. Weber, J. Electron. Mater, **20**, 179 (1991).
[20] R. Hull, J. C. Bean, L. J. Peticolas, D. Bahnck, B. E. Weir, and L. C. Feldman, Appl. Phys. Lett. **61**, 2802 (1992).
[21] $\mu_{InAs}=2.59\times10^{11}$ dyn/cm^2 *y* $\mu_{GaAs}=4.15\times10^{11}$ dyn/cm^2, $\nu_{InAs}=0.352$ *y* $\nu_{GaAs}=0.311$ from M. Neuberger, *Handbook of Electronic Materials*, in "III-V Semiconducting Compounds" (Plenum, New York, 1971), Vol. 2.
[22] S. D. Kim and J. S. Harris Jr., J. Cryst. Growth **123**, 439 (1992).
[23] S. V. Kamat and J. P. Hirth, J. Appl. Phys. **67**, 6844 (1990).

Downloaded 10 Jun 2010 to 161.116.168.169. Redistribution subject to AIP license or copyright; see http://jap.aip.org/jap/copyright.jsp